PAPER

Determination of the magnetic structure of $SmFe_3(BO_3)_4$ by neutron diffraction: comparison with other $RFe_3(BO_3)_4$ iron borates

To cite this article: C Ritter *et al* 2012 *J. Phys.: Condens. Matter* **24** 386002

J. Phys.: Condens. Matter **24** (2012) 386002 (8pp) doi:10.1088/0953-8984/24/38/386002

Determination of the magnetic structure of $SmFe_3(BO_3)_4$ by neutron diffraction: comparison with other $RFe_3(BO_3)_4$ iron borates

C Ritter[1], A Pankrats[2], I Gudim[2] and A Vorotynov[2]

[1] Institute Laue-Langevin, BP 156, F-38042 Grenoble, France
[2] L V Kirenskii Institute of Physics, Siberian Branch of RAS, Krasnoyarsk 660036, Russia

E-mail: ritter@ill.fr

Received 1 June 2012, in final form 9 August 2012
Published 24 August 2012
Online at stacks.iop.org/JPhysCM/24/386002

Abstract
Temperature dependent neutron diffraction studies were performed on $SmFe_3.BO_3/_4$. The crystallographic structure was determined to stay as *R*32 over the whole studied temperature range of 2 K < *T* < 300 K. A magnetic phase transition characterized by the magnetic propagation vector = [0 0 3=2] takes place at $T_N = 34$ K. The magnetic structure sees an easy-plane arrangement within the trigonal basal *a*–*b*-plane of ferromagnetic layers of iron and samarium having a canting angle of about 70° relative to each other. Neighbouring layers in the *c*-direction are antiferromagnetically coupled; at 2 K the magnetic moment values amount to $_{Fe} = 4{:}2.1/_B$ and $_{Sm} = 0{:}8.2/_B$. The non-Brillouin type increase of the iron magnetic moment below T_N points to a strong Fe–Sm exchange and to the simultaneous appearance of long range magnetic order on both sublattices.

(Some figures may appear in colour only in the online journal)

1. Introduction

Rare-earth iron borates, $RFe_3.BO_3/_4$, have recently been at the centre of interest due to their highly interesting structural and magnetic behaviour [1, 2]. Primarily the discovery of multiferroic properties in $GdFe_3.BO_3/_4$ [3] and $NdFe.BO_3/_4$ [4] triggered this interest. Spin reorientations were found in R = Gd [5, 6] and Ho [7] compounds and connected to the competition between the anisotropies of the iron and the rare-earth magnetic sublattice. A colossal magnetodielectric effect was found in $SmFe_3.BO_3/_4$ [8] and in reduced form in $HoFe_3.BO_3/_4$ [9] where it was linked to details of the magnetic structure. Meta-magnetism found in $TbFe_3.BO_3/_4$ [10] indicated the existence of a spin flop transition.

Crystallizing in the noncentrosymmetric trigonal space-group *R*32 a structural transition to $P3_121$ can take place on cooling at a temperature depending linearly on the rare-earth ionic radius [11, 12]. While in $ErFe_3.BO_3/_4$ ($r_{Er}3+ = 0{:}89$ Å) this transition is found above 520 K [13], $EuFe_3.BO_3/_4$ ($r_{Eu}3+ = 0{:}947$ Å) sees it at about 80 K [11]. $SmFe_3.BO_3/_4$ ($r_{Sm}3+ = 0{:}96$ Å) seems to be at the borderline of keeping the *R*32 structure even at the lowest temperatures like all the other $RFe_3.BO_3/_4$ compounds containing an even lighter rare-earth. In *R*32 the structure consists of edge sharing FeO_6 octahedra running along the crystallographic *c*-axis forming helicoidal chains of iron ions which are well separated from each other within the basal *a*–*b*-plane [14]. Triangular BO_3 groups assure the interconnection between these helicoidal chains; however, the in-plane Fe–Fe distances are at about 4.4 Å significantly longer than the intrachain Fe–Fe distance of about 3.2 Å. The rare-earth is found in the same *a*–*b*-layer as the iron atoms and sees a trigonal prismatic surrounding formed by six oxygen ions belonging to six different BO_3 groups positioned in the *a*–*b*-layers above and below. There are no direct R–O–R interactions and the corresponding

$RAl_3.BO_3/_4$ compounds do not develop any long range magnetic order [15]. The structural transition to $P3_121$ leads to minor modifications of the structure; only the equivalence between the three helicoidal chains of Fe atoms contained in the unit cell gets lost with one of these chains being slightly displaced in *c*-direction [12]. Detailed descriptions and pictures of the structures can be found in [12, 14].

Magnetic long range order develops in these $RFe_3.BO_3/_4$ compounds at temperatures between about 40 K (R = Er) and 23 K (R = La) depending again on the ionic radius of the R^{3+} involved [11]. Up to now, all studies have shown that both the iron and the rare-earth sublattice become magnetic at the same temperature. In the absence of direct magnetic R–R interactions it is assumed that the magnetic moment on the rare-earth site is induced through the polarization of the iron sublattice [6]. This can be deduced, e.g., from the non-Brillouin type behaviour of the iron sublattice magnetization as determined from neutron diffraction data [10, 13] or even more directly from the temperature dependence of the ground doublet splitting of R^{3+} as seen in spectroscopic data which reflects the strength of the R–Fe exchange coupling [16, 17]. The magnetic order is of the antiferromagnetic type with a magnetic propagation vector of = [0 0 3=2] in *R*32 (corresponding to = [0 0 1=2] in $P3_121$) [18, 10].

While susceptibility measurements or optical spectroscopy data are able to predict an overall easy-axis (along the crystallographic *c*-direction) or easy-plane orientation of the magnetic spins only neutron diffraction data allow the relative orientation and magnetic moment values of the two magnetic sublattices to be determined in detail. Neutron data exist for R = Nd, Tb, Ho, Y, Pr, Er and Dy [18, 10, 7, 13, 19] and lead to a general picture where the easy-plane anisotropy of the iron sublattice as found in $YFe_3.BO_3/_4$ is overruled by the easy-axis anisotropy of the rare-earth for R = Tb, Dy and Pr right at T_N. For R = Ho an easy-plane orientation is found between T_N and about 5 K, the temperature where the easy-axis anisotropy of the Ho-sublattice overcomes the easy-plane anisotropy of the iron sublattice leading to a spin reorientation. For R = Nd and Er the easy-plane anisotropy dominates in the whole temperature range below T_N. With respect to the single ion anisotropy of the rare-earths similar behaviour of the R = Pr, Tb, Dy and Ho ($T < 5$ K) is expected as they all have the same oblate real space shape of the 4f electrons. Expected as well is the different behaviour of $ErFe_3.BO_3/_4$ as the 4f electrons of Er^{3+} adopt a prolate shape. Unexpected is, however, the easy-plane orientation found for $NdFe_3.BO_3/_4$ which in first approximation should adopt as well an easy-axis orientation due to the oblate shape of the Nd 4f electrons. In this context it would be interesting to extend the highly interesting detailed optical spectroscopy studies as performed by Chukalina *et al* on the R = Nd (easy-plane) [16] and Popova *et al* on the R = Pr, Tb (easy-axis) [20, 17] compounds to another $RFe_3.BO_3/_4$ compound adopting an easy-plane orientation of the magnetic moments in order to determine experimentally the crystal field splitting induced by the trigonal prismatic coordination of the R^{3+} ions by oxygen.

First density functional theory (DFT) calculations on the spin exchange interactions were performed by Lee *et al* [21] for $TbFe_3.BO_3/_4$: the most interesting result of their calculations resides in the information that contrary to what could have been intuitively guessed it is not the short intrachain super-exchange Fe–O–Fe interaction (Fe–Fe ≈ 3.2 Å) which is the strongest antiferromagnetic interaction but one of the longer interchain super-super-exchange interactions Fe–O–O–Fe (Fe–Fe ≈ 4.4 Å) through a BO_3 group. This explains readily why there are, despite the presence of well separated helicoidal Fe-chains, no signs of low dimensional magnetic behaviour. These results of Lee *et al* have to be compared with the nice work of Volkov *et al* [22–25] who described the magnetic properties of several $RFe_3.BO_3/_4$ compounds using a crystal field model for the R ion and a molecular field approximation. Their calculations showed that the intrachain Fe–Fe interactions should be about twice as strong as the interchain interactions. This apparent contradiction to the results of Lee *et al* [21] could reside in the fact that contrary to Lee *et al* the model of Volkov *et al* did not differentiate between the three geometrically (Fe–O–O–Fe angles) very different interchain interactions.

Neutron diffraction studies allowed determination of the relative orientation of the iron and the rare-earth sublattices as being parallel within the *a*–*b*-layer for R = Pr [13] and antiparallel for R = Tb, Dy, Ho and Er [10, 19, 7, 13]. For $NdFe_3.BO_3/_4$ a first neutron study [18] proposed a canted arrangement of Nd and Fe spins while a more recent study [26] concluded on their parallel arrangement. The parallel alignment would be in line with an interpretation where a ferromagnetic exchange interaction between the iron 3d and the spin part of the total moment $J = S + L$ of the rare-earth would lead through the spin–orbit coupling to an antiparallel alignment of the 4f electrons relative to the iron spins for light rare-earths and a parallel alignment for heavy rare-earths [20]. One has to realize that the here discussed indirect Fe–O–R exchange interactions are coupling iron and rare-earth moments of neighbouring *a*–*b*-planes.

Further details of the magnetic structures as determined by neutron diffraction include the existence of a slight incommensurability in $NdFe_3.BO_3/_4$ below $T = 25$ K [18, 26] and the formation of a small 120° type basal plane component of the Dy magnetic moment below $T = 20$ K in $DyFe_3.BO_3/_4$ [19]. As a slight incommensurability had as well been found from resonant x-ray scattering studies above the spin reorientation transition in $GdFe_3.BO_3/_4$ [27] it is tempting to guess that diffraction studies using very high resolution could as well discover a similar incommensurability in other $RFe_3.BO_3/_4$ compounds adopting an easy-plane orientation of the magnetic moments (e.g. R = Er or Ho for $T > 5$ K). In this context one has to mention the discussion about a possible symmetry reduction in $RFe_3.BO_3/_4$ compounds below the $R32 \rightarrow P3_121$ transition: hard x-ray scattering experiments [28] have in fact found in $RFe_3.BO_3/_4$ compounds with R = Tb, Gd and Y below the structural transition temperature the presence of very weak (0 0 1) and (0 0 2) reflections which are forbidden in the assumed $P3_121$ symmetry spacegroup. Optical spectroscopy

data [17] did on the other hand not show any signs of a structural distortion below the $P3_121$ symmetry; powder neutron diffraction is not sensitive enough to see superlattice reflections of such low intensity. The 120° type arrangement of the Dy spins within the basal plane had been already found in $HoFe_3.BO_3/_4$ ($T < 5$ K) [7] and in about 10% of the sample volume in $ErFe_3.BO_3/_4$ [13] and points to the growing importance at lower temperatures of R–R interactions probably of R–O–Fe–O–R type.

Due to the very high absorption cross section of natural Sm the compound $SmFe_3.BO_3/_4$ has not been yet the subject of a neutron diffraction study. While optical absorption spectra [29] have already established a probable easy-plane type magnetic structure it is important to determine through a direct magnetic diffraction study the exact orientation of the two magnetic sublattices relative to each other and to the crystallographic unit cell as well as to determine the magnetic moment values on the iron and the samarium sites. The recent classification of $SmFe_3.BO_3/_4$ as multiferroic [30] showing, e.g., a colossal magnetodielectric effect [8] supports further the need for a neutron study of the magnetic structure. We will present in this work our results on a powder neutron diffraction experiment on $SmFe_3.BO_3/_4$, discussing and relating them to previous results on $RFe_3.BO_3/_4$ compounds.

2. Experimental details

2.1. Sample preparation

Single crystals of $SmFe_3.BO_3/_4$ were prepared at the Institute of Physics at Krasnoyarsk following the preparation procedure described in detail in [31]. Due to the strong neutron absorption of natural boron 99% with ^{11}B enriched B_2O_3 was used. Powder samples for the neutron measurements were prepared from the grown crystals by grinding.

2.2. Neutron diffraction measurements

There exist at least five different possibilities to circumvent or overcome the extremely high neutron absorption of natural samarium. (1) Using hot neutrons with a very short neutron wavelength it is possible to reduce the absorption cross section; however, at the expense of a strongly reduced resolution [32]. (2) Preparing the compound using a less absorbing isotope like ^{154}Sm [33], a solution no longer conceivable due to the prohibitively high price of these isotopes. (3) Using a specially designed large-area single crystal flat-plate sample holder reducing the thickness of the sample to a minimum while increasing its surface area [34]. (4) Using a cylindrical double wall container to reduce the thickness of the sample in the beam to an acceptable value. This last option calls for a distance between the walls of the container of less than a 0.3 mm while keeping a diameter of about 1 cm. It would be technically very difficult to fabricate such a double wall container and it would be nearly impossible to fill it homogeneously with the powder. (5) Mixing the absorbing powder sample with Al powder [35]. The additional

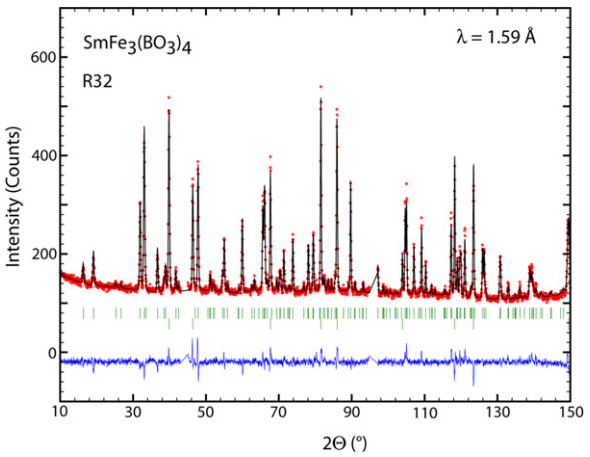

Figure 1. Observed (dots, red), calculated (line, black) and difference patterns of $SmFe_3.BO_3/_4$ at room temperature in the paramagnetic state refined in *R*32. The tick marks indicate the calculated positions of the Bragg peaks of the main phase (upper row) and the secondary Al phase (lower row).

powder Bragg peaks caused by the Al powder are few in number and can be adequately taken into account when making Rietveld refinements.

In the case of our study on $SmFe_3.BO_3/_4$ we chose to use a double wall container having a diameter of 1 cm and 1 mm distance between the walls into which we filled the finely powdered sample which had been additionally mixed with about 10 parts of Al powder for one part of $SmFe_3.BO_3/_4$ powder.

Neutron diffraction data were taken at the Institut Laue-Langevin in Grenoble, France, using the high resolution powder diffractometer D2B (= 1.594 Å) and the high flux powder diffractometers D20 (= 2.422 Å, 1.81 Å) and D1B (= 2.52 Å). The high resolution data were taken at room temperature measuring for about 5 h. High intensity data on D1B were measured at 50 and 1.5 K for 1 h each. The temperature dependence of the neutron diffractogram (thermodiffractogram) was recorded on D20 between 1.7 and 50 K taking spectra of about 30 min every 1.4 K in order to study in detail the magnetic phase transition. For this measurement the sample had not yet been diluted with Al powder. Additional data sets were taken at 50 and 1.7 K on D20 using the high resolution setup in order to search for any symmetry reduction at low temperatures.

All data were refined by the Rietveld method using the FULLPROF [36] program. The added Al powder was included in the refinements as the secondary phase.

3. Results and discussion

The high resolution data taken at room temperature were refined using the spacegroup *R*32. Apart from the added Al powder and two lines from the vanadium sample container no impurities were present. Figure 1 shows a plot of the refinement and table 1 shows the resulting atom coordinates and some interatomic distances. According to

Table 1. Lattice constants, atomic coordinates in *R*32 and interatomic distances of $SmFe_3.BO_3/_4$ at room temperature.

a (Å)		9.5663(1)
c (Å)		7.5896(2)
Sm (3a)		
Fe (9d)	*x*	0.5503(3)
O1 (9e)	*x*	0.8564(8)
O2 (9e)	*x*	0.5922(6)
O3 (18f)	*x*	0.0273(4)
	y	0.2144(4)
	z	0.1837(5)
B1 (3b)		
B2 (9e)	*x*	0.4462(6)
6 × Sm–O3 (Å)		2.384(4)
2 × Fe–O1 (Å)		2.0281(8)
2 × Fe–O2 (Å)		2.035(5)
2 × Fe–O3 (Å)		1.952(5)
Fe–Fe (Å)		3.181(2)
R_{Bragg}		7.6

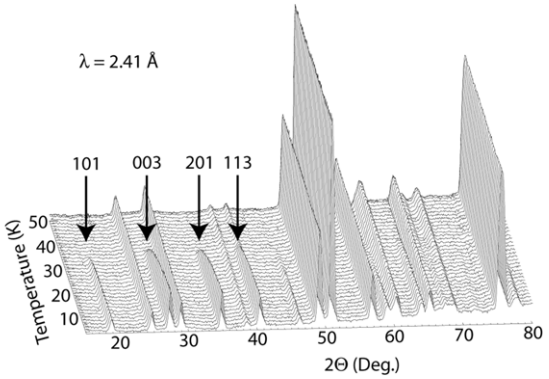

Figure 2. Thermal dependence of the neutron diffraction pattern of $SmFe_3.BO_3/_4$ between 1.5 and 50 K showing the appearance of magnetic Bragg peaks at about 35 K. The magnetic peaks are indexed in a unit cell doubled in the *c*-direction.

Hinatsu *et al* [11] a structural transition from *R*32 to $P3_121$ could take place in $SmFe_3.BO_3/_4$ at very low temperatures. This structural transition would be characterized through the appearance of additional Bragg peaks of very small intensity. D20 is the perfect diffractometer to search for these new Bragg peaks due to its very high neutron flux. Data taken at 50 K in the paramagnetic phase and at 1.7 K in the magnetically ordered phase did not show any sign of additional structural Bragg peaks and allow us to exclude any structural transition down to the base temperature. This is in accordance with the spectroscopic data of Chukalina *et al* [29].

Figure 2 displays the thermodiffractogram of $SmFe_3.BO_3/_4$ taken on D20 between 1.7 and 50 K. The appearance of additional, relatively strong reflections of magnetic origin at low angles at about 35 K can clearly be seen. Fitting the intensity of the most intense magnetic peaks the magnetic transition temperature was determined to be $T_N = 34$ K and no signs of a spin reorientation or of a non-steady behaviour were found.

All magnetic peaks can be indexed using the magnetic propagation vector = [0 0 3=2] which had been already found in other $RFe_3.BO_3/_4$ compounds (R = Pr, Nd) [13, 18] which keep the *R*32 structure at low temperatures. This propagation vector leads to a doubling of the magnetic unit cell in the *c*-direction as compared to the original crystallographic cell. The indices shown in figure 2 are based, therefore, on a cell doubled in the *c*-direction; they can be directly compared as well to magnetic peaks in the other $RFe_3.BO_3/_4$ compounds adopting at low temperatures the $P3_121$ structure which see the same doubling in the *c*-direction through the magnetic propagation vector = [0 0 1=2]. The position and the intensity of these new peaks resemble strongly those found in the compound $YFe_3.BO_3/_4$ [7] where the refinement concluded on a magnetic structure with the Fe spins aligned within the trigonal basal plane. In order to profit from the highest possible sensitivity for the magnetic scattering the determination of the magnetic structure of $SmFe_3.BO_3/_4$ was made by refining the difference spectrum 2–50 K recorded on the high intensity diffractometer D1B which represents the purely magnetic scattering of the compound. The only refinable parameters are the background parameters and the magnetic moment values of the magnetic sites. The scale factor has to be kept fixed to the value found from a refinement of the non-magnetic spectrum taken at 50 K. While the magnetic form factor of Fe^{3+} is well known and tabulated the same is not true for the case of the rare-earths where the magnetic form factor $f.Q/$ depends strongly on the ratio between the spin and the orbital moment. In the dipolar approximation the magnetic form factor can be expressed as $f.Q/ = \langle j_0\rangle + c_2\langle j_2\rangle$, with $\langle j_n\rangle$ representing the integrals of the product of the 4f radial electron wave function and the spherical Bessel function of order *n* and $c_2 = J.J+1/+L.L+1/-S.S+1/=.3J.J+1/+S.S+1/-L.L+1//$.

Assuming a strong spin–orbit splitting one has to consider only the ground state multiplet which in the case of the $4f^5$ ion Sm^{3+} is represented by the term $^6H_{5=2}$ with $S = 5=2; L = 5$ and $J = 5=2$ giving $c_2 = 6$. As $\langle j_2\rangle$ grows with increasing scattering angle this leads to the special situation where the resulting magnetic form factor has a maximum at about sin 2 = = 0:37 $Å^{-1}$, e.g. magnetic scattering intensity of Sm^{3+} could be present at high scattering angles. As, however, $c_2 =$ L= Total = L=. L + S/, where L is the orbital, S the spin and Total the total magnetic moment, one can see that the expected total magnetic moment which is the quantity measurable in the powder neutron diffraction experiment should be small for large c_2. Using values tabulated in [37] $\langle j_0\rangle$ and $\langle j_2\rangle$ were determined as functions of sin 2 = and $f.Q/$ calculated for $c_2 = 6$.

Using the same magnetic structure model as already found for $YFe_3.BO_3/_4$ [7] and $ErFe_3.BO_3/_4$ [13] below T_N and for $HoFe_3.BO_3/_4$ for $T_N > T > 5$ K [7] the refinement of the difference spectrum (figure 3) converged rapidly. This magnetic structure sees the magnetic moments of all iron sites within the same trigonal *a*–*b*-layer ferromagnetically aligned with an antiferromagnetic alignment between neighbouring layers. The same is true for the Sm sites which are in this

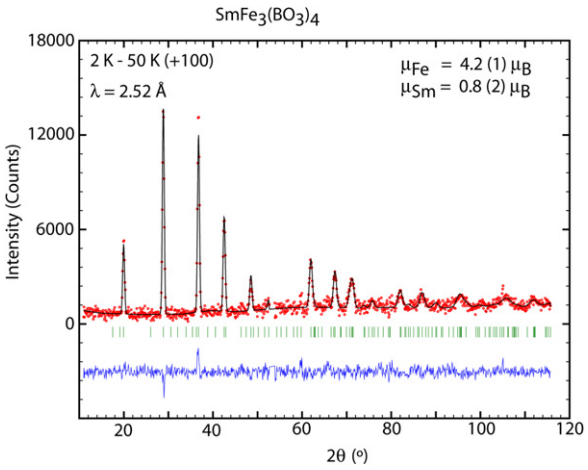

Figure 3. Refinement of the difference spectrum 2–50 K of $SmFe_3.BO_3/_4$. Observed (dots, red), calculated (line, black) and difference patterns.

model furthermore oriented parallel to the iron moments. The magnetic moment values amount to $_{Fe} = 4{:}2.1/\ _B$ and $_{Sm} = 0{:}24.4/\ _B$ at 1.7 K. Forcing the magnetic moment value on the Sm-site (1) to assume an antiparallel alignment to the iron sublattice or (2) to be zero, we verified the sensitivity of the refinement to these possibilities: while a refinement with the parallel alignment results in a magnetic *R*-factor of $R_{Mag} = 9{:}7\%$, assuming no magnetic moment on the Sm-site gives $R_{Mag} = 10{:}5\%$, while the antiparallel alignment gives $R_{Mag} = 12{:}8\%$. A parallel orientation of the iron and the samarium sublattices could be expected as it corresponds to the situation already found in $PrFe_3.BO_3/_4$ and $NdFe_3.BO_3/_4$ [13, 26], the only other $RFe_3.BO_3/_4$ compounds with light rare-earths for which neutron data are available. We then, however, verified whether any canting between the iron and the rare-earth sublattices as originally proposed for $NdFe_3.BO_3/_4$ [18] existed and found that a refinement allowing the canting converged slowly to magnetic moments of $_{Fe} = 4{:}2.1/\ _B$ and $_{Sm} = 0{:}8.2/\ _B$, giving a final $R_{Mag} = 9{:}1\%$ and a canting angle of about 70°. Analysing the refinement more deeply it was found that all refinements with a total samarium moment in the range $0{:}5\ _B < _{Total} < 1{:}4\ _B$ are able to refine the data nicely, but that in all cases a canting between 90° and 60° between the iron and the samarium sublattices is favoured against a collinear parallel arrangement. Due to the trigonal symmetry it is not possible to determine the absolute spin direction within the basal plane from powder diffraction data as the magnetic reflections containing the needed information appear at identical 2θ values. Figure 4 displays the magnetic structure of $SmFe_3.BO_3/_4$; the magnetic moment of the Sm-site has been up-scaled by a factor 2 to aid its visibility.

In distinction from $HoFe_3.BO_3/_4$ (for $T_N > T > 5$ K) [7] and $ErFe_3.BO_3/_4$ [13] there is no inclination from the pure basal plane orientation into the *c*-direction. This makes $SmFe_3.BO_3/_4$, apart from $NdFe_3.BO_3/_4$ where the collinearity of the iron and the rare-earth sublattices is as well still a matter of discussion, the only $RFe_3.BO_3/_4$ compound possessing a purely basal plane type magnetic structure. As already mentioned above it is not possible to deduce from these powder data the presence or absence of a slight incommensurability as found in the R = Nd and Gd compounds.

Knowing the magnetic structure we determined the thermal evolution of the iron magnetic moment by refining sequentially the high intensity data taken between 1.7 and 50 K (figure 5). As the data of the thermal scan did not have the same quality as the difference spectrum from which the details of the samarium sublattice were refined we fixed the samarium magnetic moment value to zero for this sequential refinement in order to avoid any correlation effects.

As already found for some other $RFe_3.BO_3/_4$ compounds [10, 13, 19] with magnetic R, the thermal dependence of the magnetic moment of Fe^{3+} does not follow the

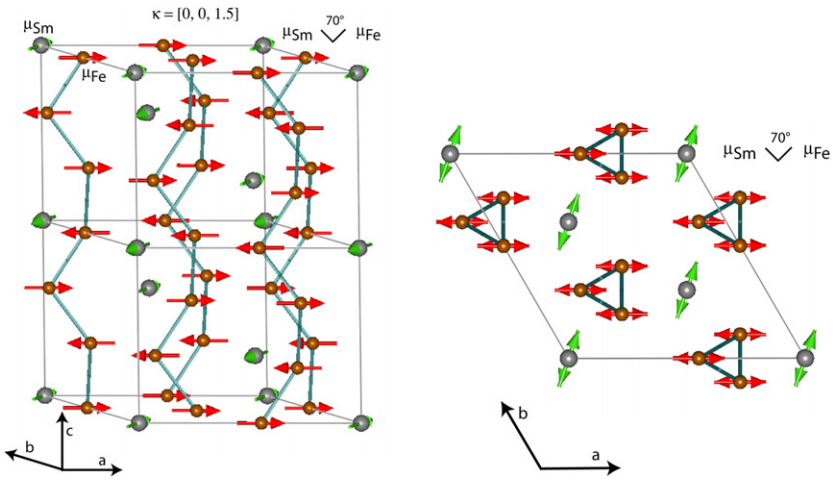

Figure 4. The magnetic structure of $SmFe_3.BO_3/_4$. Sm-moments are shown in green, Fe-spins in red, the direct Fe–Fe-exchange along the helicoidal chains is indicated by light blue lines. Left: view along the *c*-direction showing the doubling of the crystallographic unit cell. Right: view of the *a*–*b*-plane showing the canting between the Sm- and Fe-sublattices.

Table 2. Details of the magnetic structures adopted in $RFe_3.BO_3/_4$ compounds. Sg: = spacegroup; = magnetic propagation vector, Anis = anisotropy, EP = easy-plane, EA = easy-axis.

R	Sg.		Anis.	Alignment, canting	Reference
(Y)	$P3_121$	[0 0 1=2]	EP	—	[7]
Pr	$R32$	[0 0 3=2]	EA	↑↑	[13]
Nd	$R32$	[0 0 3=2] ($T_N > T > 13{:}5$ K) [0 0 3=2 + "] ($T < 13{:}5$ K)	EP EP	↑↑ ? 0° or 70° ↑↑	[18, 26]
Sm	$R32$	[0 0 3=2]	EP	.↑↑/ ≈ 70° in plane	This work
Gd	$P3_121$	[0 0 1=2 + "] .$T_N > T > 10$ K/ [0 0 1=2] (10 K < T < 9 K) (9 K > T)	EP EP EA	? ≈ 45° Gd, Fe variable with T ? ≈ 45° Fe, Gd in c-dir. ?	[27]
Tb	$P3_121$	[0 0 1=2]	EA	↑↓	[10]
Dy	$P3_121$	[0 0 1=2]	EA	↑↓ 12°, (Dy: 120°)	[18]
Ho	$P3_121$	[0 0 1=2] .$T_N > T > 5$ K/ .$T < 5$ K/	EP EA	↑↓ 28° .Fe_2; $T = 6$ K/ in c-dir. ↑↓ 22° (Ho: 120°)	[7]
Er	$P3_121$	[0 0 1=2]	EP	↑↓ 14° (Fe) in c-dir. 10%: Er, 120°	[13]

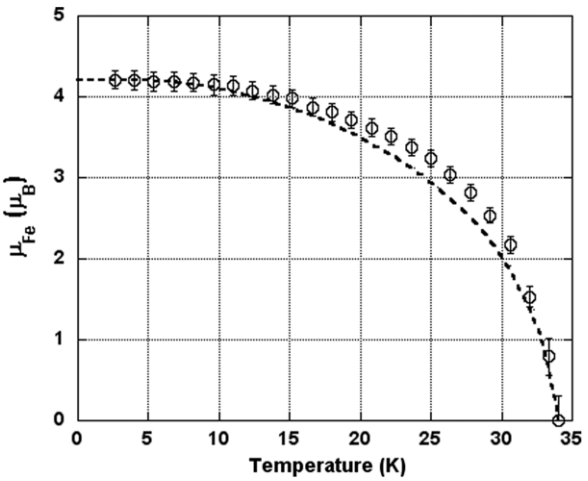

Figure 5. The temperature dependence of the magnetic moment value of Fe in $SmFe_3.BO_3/_4$. The dashed line represents a fit of the data with a Brillouin function with $J = 5{=}2$.

Brillouin-type behaviour of an $S = 5{=}2$ ion. This had been interpreted as indicating the influence of the Fe–R-exchange interactions polarizing the rare-earth sublattice and should here as well point to the occurrence of a significant magnetic moment on the samarium site immediately below T_N induced by the Fe-sublattice. We would like to recall that a total magnetic moment of about $_{Total} = _{Sm} = 0{:}8$ $_B$ as determined from the neutron refinement reflects—assuming $c_2 = 6$, as used for the refinement—an orbital moment of about $_L = c_2 \times 0{:}8$ $_B = 4{:}8$ $_B$ and a spin moment of $_S = _L - _{Total} = 4{:}8$ $_B - 0{:}8$ $_B = 4$ $_B$. A nice Brillouin-type behaviour had been found in $YFe_3.BO_3/_4$ [10] where the rare-earth site is occupied by non-magnetic yttrium.

Table 2 lists the information available up to now on the detailed magnetic structures adopted in $RFe_3.BO_3/_4$ compounds. It becomes apparent that once a simple classification of the anisotropy into easy-axis (EA) and easy-plane (EP) arrangements has been made one has to further specify first the alignment between the iron and the rare-earth sublattice according to a parallel (↑↑) and or an antiparallel (↑↓) orientation and secondly according to a possible canting from the main anisotropy direction. $SmFe_3.BO_3/_4$ resembles strongly $NdFe_3.BO_3/_4$ in as far as both compounds see an easy-plane anisotropy and no canting of a sublattice towards the c-direction. The two $RFe_3.BO_3/_4$ compounds which undergo in zero magnetic field a spin reorientation as a function of temperature, namely $GdFe_3.BO_3/_4$ and $HoFe_3.BO_3/_4$, see already a significant canting of the iron (R = Ho) or of both sublattices (R = Gd) towards the c-direction above the spin reorientation temperature within the easy-plane state. In $SmFe_3.BO_3/_4$, as in $NdFe_3.BO_3/_4$ [30], a strong spontaneous polarization is seen in the basal plane below T_N while in $HoFe_3.BO_3/_4$ [9] it is strong as well along the c-axis; this conforms to the details of the magnetic structures. A canting between the iron and the rare-earth sublattice within the basal plane, likely to exist in $SmFe_3.BO_3/_4$, has not been found in the other studied easy-plane $RFe_3.BO_3/_4$ compounds. It might, however, be present in $NdFe_3.BO_3/_4$ where powder [18] and single crystal [26] data gave contradicting results. We would like to mention in this context that the value found in the single crystal study for the magnetic moment of Nd is surprisingly small with $_{Nd} = 1{:}1$ $_B$.

Further studies will certainly concentrate on $RFe_3.BO_3/_4$ compounds adopting the easy-plane magnetic structures as the multiferroic properties of the easy-axis ferroborates are far less interesting [2]. First attempts to control the magneto-electric properties of these compounds by mixing easy-plane and easy-axis type rare-earths resulted in interesting but partly surprising results. While in $Tb_{1-x}Er_xFe_3.BO_3/_4$ [38] the easy-axis state is kept down to lowest temperatures even for $x = 0{:}75$, in $Nd_{1-x}Dy_xFe_3.BO_3/_4$ [39] the substitution of 25% of Nd by Dy can successfully introduce a temperature dependent spin reorientation from easy-plane to easy-axis at the relatively high temperature of 25 K. Knowing that $NdFe_3.BO_3/_4$ adopts the easy-plane type magnetic structure the substitution of 50% Ho by Nd in $Ho_{0:5}Nd_{0:5}Fe_3.BO_3/_4$

should in theory push the spin reorientation from easy-plane to easy-axis as found in pure $HoFe_3.BO_3/_4$ at 5 K to even lower temperatures. Surprisingly it was found that in $Ho_{0:5}Nd_{0:5}Fe_3.BO_3/_4$ this spin reorientation shifts up in temperature to 9 K [9]. This shows that the simple picture of a competition between the axial and the planar anisotropy of the rare-earths is not sufficient to explain the details of the magnetic structures adopted. Due to the strong resemblance of the magnetic structures adopted by $NdFe_3.BO_3/_4$ and the here studied $SmFe_3.BO_3/_4$, mixed $R_{1-x}Sm_xFe_3.BO_3/_4$ compounds seem to be promising candidates when trying to elucidate these details.

4. Summary

High resolution and temperature dependent high intensity powder neutron diffraction studies on $SmFe_3.BO_3/_4$ revealed the persistence of the trigonal structure *R*32 down to very low temperatures (2 K) and the formation of an easy-plane type magnetic structure with $= [0\,0\,3{=}2]$ below $T_N = 34$ K. From the non-Brillouin type increase of the iron magnetic moment below T_N a strong interaction between the iron and the samarium sublattices leading to the simultaneous appearance of long range magnetic order is deduced. At 2 K the magnetic moment values amount to $_{Fe} = 4{:}1.1/\ _B$ and $_{Sm} = 0{:}8.2/\ _B$. Within the basal plane of the trigonal structure the sublattices of iron and samarium are each ferromagnetically ordered while the coupling to the neighbouring layers in the *c*-direction is antiferromagnetic. The two sublattices are not collinear but adopt a canting angle of about 70° to each other. As there is no magnetic moment component pointing in the *c*-direction $SmFe_3.BO_3/_4$ is only the second $RFe_3.BO_3/_4$ compound after $NdFe_3.BO_3/_4$ to show a purely easy-plane type magnetic structure.

Acknowledgment

This work was supported by RFBR, grant No. 10-02-00765.

References

[1] See e.g. Fausti D, Nugroho A A, van Loosdrecht P H M, Klimin S A, Popova M N and Bezmaternykh L N 2006 *Phys. Rev.* B **74** 024403
Vasiliev A N and Popova E A 2006 *Low Temp. Phys.* **32** 735
[2] Kadomtseva A M *et al* 2010 *Low Temp. Phys.* **36** 511
[3] Zvezdin A K, Krotov S S, Kadomtseva A M, Vorob'ev G P, Popov Yu F, Pyatokov A P, Bezmaternykh L N and Popova E A 2005 *JETP Lett.* **81** 335
[4] Zvezdin A K, Vorob'ev G P, Kadomtseva A M, Popov Yu F, Pyatakov A P, Bezmaternykh L N, Kuvardin A V and Popova E A 2006 *JETP Lett.* **83** 509
[5] Levitin R Z, Popova E A, Chtsherbov R M, Vasiliev A N, Chukalina E P, Klimin S A, van Loosdrecht P H M, Fausti D and Bezmaternykh L N 2004 *JETP Lett.* **79** 423
[6] Pankrats A I, Petrakovskii G A, Bezmaternykh L N and Bayukov O A 2004 *JETP* **99** 766
[7] Ritter C, Vorotynov A, Pankrats A, Petrakovskiĭ G, Temerov V, Gudim I and Szymczak R 2008 *J. Phys.: Condens. Matter* **20** 365209
[8] Mukhin A A, Vorob'ev G P, Ivanov V Yu, Kadomtseva A M, Narizhnaya A S, Kuz'menko A M, Popov Yu F, Bezmaternykh L N and Gudim I A 2011 *JETP Lett.* **93** 275
[9] Chaudhury R P, Yen F, Lorenz B, Sun Y Y, Bezmaternykh L N, Temerov V L and Chu C W 2009 *Phys. Rev.* B **80** 104424
[10] Ritter C, Balaev A, Vorotynov A, Petrakovskiĭ G, Velikanov D, Temerov V and Gudim I 2007 *J. Phys.: Condens. Matter* **19** 196227
[11] Hinatsu Y, Doi Y, Ito K, Wakeshima M and Alemi A 2003 *J. Solid State Chem.* **172** 438
[12] Klimin S A, Fausti D, Meetsma A, Bezmaternykh L N, van Loosdrecht P H M and Palstra T T M 2005 *Acta Crystallogr.* B **61** 481
[13] Ritter C, Vorotynov A, Pankrats A, Petrakovskiĭ G, Temerov V, Gudim I and Szymczak R 2010 *J. Phys.: Condens. Matter* **22** 206002
[14] Campa J A, Cascales C, Gutiérrez-Puebla E, Monge M A, Rasines I and Ruíz-Valero C 1997 *Chem. Mater.* **9** 237
[15] Neogy D, Chattopadhay K N, Chakrabarti P K, Sen H and Wanklyn B M 1996 *J. Magn. Magn. Mater.* **154** 127
Neogy D, Chattopadhay K N, Chakrabarti P K, Sen H and Wanklyn B M 1997 *J. Phys. Chem. Solids* **59** 783
[16] Chukalina E P, Kuritsin D Yu, Popova M N, Bezmaternykh L N, Kharlamova S A and Temerov V L 2004 *Phys. Lett.* A **322** 239
[17] Popova M N, Stanislavchuk T N, Malkin B Z and Bezmaternykh L N 2012 *J. Phys.: Condens. Matter* **24** 196002
[18] Fischer P *et al* 2006 *J. Phys.: Condens. Matter* **18** 7975
[19] Ritter C, Pankrats A, Gudim I and Vorotynov A 2012 *J. Phys. Conf. Ser.* **340** 012065
[20] Popova M N, Stanislavchuk T N, Malkin B Z and Bezmaternykh L N 2009 *Phys. Rev.* B **80** 195101
[21] Lee C, Kang J, Lee K H and Whangbo M-H 2009 *Chem. Mater.* **21** 2534
[22] Popova E A *et al* 2007 *Phys. Rev.* B **75** 224413
[23] Volkov D V, Demidov A A and Kolmakova N P 2007 *JETP* **104** 897
[24] Volkov D V, Demidov A A and Kolmakova N P 2008 *JETP* **106** 723
[25] Demidov A A and Volkov D V 2011 *Phys. Solid State* **53** 985
[26] Janoschek M, Fischer P, Schefer J, Roessli B, Pomjakushin V, Meven M, Petricek V, Petrakovskiĭ G and Bezmaternykh L 2010 *Phys. Rev.* B **81** 094429
[27] Mo H, Nelson C S, Bezmaternykh L N and Temerov V T 2008 *Phys. Rev.* B **78** 214407
[28] Hamann-Borrero J E, Philipp M, Kataeva O, Zimmermann M v, Geck J, Klingeler R, Visiliev A, Bezmaternykh L, Büchner B and Hess C 2010 *Phys. Rev.* B **82** 094411
[29] Chukalina E P, Popova M N, Bezmaternykh L N and Gudim I A 2010 *Phys. Lett.* A **374** 1790
[30] Popov Yu F, Pyatakov A P, Kadomtseva A M, Vorob'ev G P, Zvezdin A K, Mukhin A A, Ivanov Yu V and Gudim I A 2010 *JETP* **111** 199
[31] Gudim I A, Eremin E V and Temerov V L 2010 *J. Cryst. Growth* **312** 2427
[32] Granovsky S A, Kreyssig A, Doerr M, Ritter C, Dudzik E, Feyerherm R, Canfield P C and Loewenhaupt M 2010 *J. Phys.: Condens. Matter* **22** 226005
[33] Tomka G J, Ritter C, Riedi P C, Kapusta Cz and Kocemba W 1998 *Phys. Rev.* B **58** 6330

[34] Ryan D H, Cadogan J M, Ritter C, Canepa F, Palenzona A and Putti M 2009 *Phys. Rev.* B **80** 220503
[35] Ritter C, Cywinski R, Kilcoyne S H, Mondal S and Rainford B D 1994 *Phys. Rev.* B **50** 9894
[36] Rodriguez-Carvajal J 1993 *Physica* B **192** 55
[37] Brown P J 1992 *Magnetic Form Factors* (*International Tables for Crystallography* vol C) ed A J C Wilson (Dordrecht: Kluwer Academic)
[38] Zvezdin A K, Kadomtseva A M, Popov Yu F, Vorob'ev G P, Pyatokov A P, Ivanov V Yu, Kuz'menko A M, Muhkin A A, Bezmaternykh L N and Gudim I A 2009 *JETP* **109** 68
[39] Popov Yu F, Kadomtseva A M, Vorob'ev G P, Mukhin A A, Ivanov V Yu, Kuz'menko A M, Prokhorov A S, Bezmaternykh L N and Temerov V L 2009 *JETP Lett.* **89** 345